Biomaterials Advances 158 (2024) 213762

Contents lists available at ScienceDirect

Biomaterials Advances

journal homepage: www.journals.elsevier.com/materials-science-and-engineering-c

Co-release of nitric oxide and L-arginine from poly (β-amino ester)-based adhesive reprogram macrophages for accelerated wound healing and angiogenesis *in vitro* and *in vivo*

Parisa Heydari [a,b], Mahshid Kharaziha [a,*], Jaleh Varshosaz [c,*], Anousheh Zargar Kharazi [b,d,**], Shaghayegh Haghjooy Javanmard [b]

[a] Department of Materials Engineering, Isfahan University of Technology, Isfahan 84156-83111, Iran
[b] Applied Physiology Research Center, Isfahan, Cardiovascular Research Institute, Isfahan University of Medical Sciences, Isfahan, Iran
[c] Novel Drug Delivery Systems Research Center, Department of Pharmaceutics, School of Pharmacy and Pharmaceutical Science, Isfahan University of Medical Science, Isfahan, Iran
[d] Biomaterials Nanotechnology and Tissue Engineering Faculty, School of Advanced Technologies in Medicine, Isfahan University of Medical Sciences, Isfahan, Iran

ARTICLE INFO

Keywords:
Poly (β-amino ester)
Methacrylate poly-L-arginine
Nitric oxide
Adhesive
Chronic wound healing

ABSTRACT

Recently, insufficient angiogenesis and prolonged inflammation are crucial challenges of chronic skin wound healing. The sustained release of L-Arginine (L-Arg) and nitric oxide (NO) production can control immune responses, improve angiogenesis, enhance re-epithelialization, and accelerate wound healing. Here, we aim to improve wound healing *via* the controlled release of NO and L-Arg from poly (β-amino ester) (PβAE). In this regard, PβAE is functionalized with methacrylate poly-L-Arg (PAMA), and the role of PAMA content (50, 66, and 75 wt%) on the adhesive properties, L-Arg, and NO release, as well as collagen deposition, inflammatory responses, and angiogenesis, is investigated *in vitro* and *in vivo*. Results show that the PAMA/ PβAE could provide suitable adhesive strength (~25 kPa) for wound healing application. In addition, increasing the PAMA content from 50 to 75 wt% results in an increased release of L-Arg (approximately 1.4–1.7 times) and enhanced NO production (approximately 2 times), promoting skin cell proliferation and migration. The *in vitro* studies also show that compared to PβAE hydrogel, incorporation of 66 wt% PAMA (PAMA 66 sample) reveals superior collagen I synthesis (~ 3–4 times) of fibroblasts, controlled pro-inflammatory and improved anti-inflammatory cytokines secretion of macrophages, and accelerated angiogenesis (~1.5–2 times). *In vivo* studies in a rat model with a full-thickness skin defect also demonstrate the PAMA66 sample could accelerate wound healing (~98 %) and angiogenesis, compared to control (untreated wound) and Tegaderm™ commercial wound dressing. In summary, the engineered multifunctional PAMA functionalized PβAE hydrogel with desired NO and L-Arg release, and adhesive properties can potentially reprogram macrophages and accelerate skin healing for chronic wound healing.

1. Introduction

In chronic wounds, insufficient angiogenesis, decreasing collagen deposition, prolonged immune response, and other dysregulation can lead to "hard-to-heal" damages or nonfunctional scars [1,2]. Consequently, it is necessary to use bioactive dressings with clinical intervention to accelerate wound healing for chronic skin injuries [3,4]. Recently, immunomodulatory dressings have been introduced to simultaneously reduce inflammation response and enhance angiogenesis and collagen deposition, resulting in the expedited recovery of the wound [5,6]. These dressings are often based on bioactive polymers and hydrogels incorporated with various anti-inflammatory parameters such as natural polymer (*e.g.*, chitosan) [7], growth factors [8], peptide agent (*e.g.*, SILY, collagen I binding peptide) [9], anti-inflammation drugs (*e.g.*, Curcumin) [10], or radical nitric oxide (NO) donors, including L-arginine (L-Arg) [11,12]. L-Arg has been recently introduced as an

* Corresponding authors.
** Correspondence to: A.Z. Kharazi, Applied Physiology Research Center, Isfahan, Cardiovascular Research Institute, Isfahan University of Medical Sciences, Isfahan, Iran.
E-mail addresses: kharaziha@cc.iut.ac.ir (M. Kharaziha), varshosaz@pharm.mui.ac.ir (J. Varshosaz), a_zargar@med.mui.ac.ir (A.Z. Kharazi).

https://doi.org/10.1016/j.bioadv.2024.213762
Received 2 July 2023; Received in revised form 6 December 2023; Accepted 6 January 2024
Available online 11 January 2024

immunomodulatory agent to regulate NO production, accelerate collagen synthesis, and enhance anti-inflammatory (M2) cytokine expression [12,13]. At the wound site, L-Arg is metabolized into NO by macrophages and endothelial cells using nitric oxide synthase (NOS) which accelerates angiogenesis and collagen synthesis and controls immune responses [14,15]. However, the free form of L-Arg cannot be utilized efficiently due to its easy dissolution into the surrounding plasma rather than being concentrated at the wound site, which decreases its efficacy [16]. Conversely, uncontrolled NO production may have cytotoxic properties at high dosages [12]. In addition, continuous or burst releases of L-Arg may lead to fibrosis and unfunctional scarring [17,18]. Encapsulation [19], polymerization [20], and conjugation of L-Arg with other polymers or scaffolds [21] are the alternative strategies to control L-Arg release and NO production at wound sites. Ling et al. [14] synthesized polydopamine-functionalized chitosan hydrogels conjugating with L-Arg to control NO production, enhance blood vessel formation and, promote antibacterial activity for chronic wound healing. Zhang et al. [12] also reported that *in vivo* collagen I and III expression and scar formation in a rat model could be optimized by conjugating L-Arg to chitosan-based wound dressings. Despite significant advances in L-Arg and poly-L-Arg for wound healing application, some issues still inevitably remain. For example, it is necessary for wound dressing to have ideal mechanical properties against physiological or external forces in daily activities [22]. Poly (β-amino ester) (PβAE) with good biocompatibility, controllable biodegradability, mechanical performances, and bio functionality is widely used as a cationic and pH-sensitive polymer for tissue repair applications and gene delivery [23,24]. Recently, we synthesized PβAE with four different PβAE monomer ratios (diacrylate: diamine = 1.1:1, 1.5:1, 2:1, and 3:1) and then functionalized it with poly-L-Arg methacrylate (PAMA). We demonstrated that PβAE at the optimized diacrylate: diamine ratio (1.5:1) provided an appropriate range of mechanical, degradation rate, and swelling ratio, which could be a perfect composition for the soft tissue engineering application [25]. However, the role of PAMA content on the L-Arg and NO release, adhesive properties, and wound healing ability has not been studied.

This study aims to engineer immunomodulatory wound dressing based on PβAE incorporated with PAMA for wound healing application. In this regard, PAMA content was changed from 50 to 75 wt% to adjust NO and L-Arg release, adhesive properties, and wound healing rate. The engineered hydrogels are also examined in contact with various cell types, including L929 fibroblasts, RAW-264.7 macrophage, and human umbilical vein endothelial cells (HUVECs). The immunomodulatory properties of this hydrogel on immune cells are also investigated according to anti-inflammatory and pro-inflammatory cytokine levels. Consequently, the *in vivo* wound healing process is evaluated when PAMA/PβAE hydrogel is implanted into a skin defect in a rat model. PAMA/ PβAE hydrogel with desired properties is expected to be a suitable candidate to accelerate the regeneration and repair of chronic wounds.

2. Materials and methods

2.1. Materials and reagents

1-ethyl-3-(3-(dimethylamine) propyl) carbodiimide hydrochloride (EDC), N-hydroxysuccinimide (NHS), 2,2-dimethoxy-2-phenyl-acetophenone (DMPA), 3-(4,5-dimethylthiazol-2-yl)-2,5-diphenyltetrazolium bromide (MTT), paraformaldehyde (PFA), Triton X100, phalloidin-FITC, 4′,6-diamidino-2-phenylindole (DAPI), bovine serum albumin (BSA), lipopolysaccharide (LPS), Matrigel, Hematoxylin and eosin (H&E) stain, and dialysis tube (10 K MWCO) were purchased from Sigma-Aldrich (USA). Dichloromethane (DCM) diethyl ether, and dimethyl sulfoxide (DMSO) were obtained by Merck (Germany). Additionally, Dulbecco's Modified Eagle Medium (DMEM-high), fetal bovine serum (FBS), streptomycin, and penicillin were supplied by Bioidea (Iran). For the experimental procedures, RNA extraction, cDNA synthesis, and SYBR Green PCR kits were obtained from Biofact (Korea). Also, the Bradford protein assay kit was purchased from Partocib (Iran), and the Griess reagent kit was obtained from Natrix (Iran). Tumor necrosis factor-α (TNF-α), interleukin-6 (IL-6), interleukin-10 (IL-10), and tissue growth factor-β (TGF-β) Elisa kits were purchased from KPG (Iran). Distilled water (DDW, Bioidea) was used in all experiments.

2.2. Synthesis of PAMA/ PβAE polymers

Methacrylate poly-L-Arg (PAMA) and PβAE were synthesized, according to our previous study [25]. In order to investigate the role of PAMA content on the properties of polymers, PAMA/ PβAE polymers with various PAMA: PβAE weight ratios of 1:1, 2:1, and 3:1 were made by mixing 1 wt%, 2 wt%, and 3 wt% aqueous PAMA solutions with 1 wt % PβAE solutions. Subsequently, the polymer solution was mixed with EDC and NHS, stirring at 4 °C for 4 h. The mass ratio of EDC: NHS to the polymer blend (PβAE + PAMA) was maintained at 1:1:12. Then, the solutions were subjected to dialysis against deionized water (DDW) using a cellulose dialysis membrane with a cutoff of 10 kDa. This process aimed to remove any remaining traces of EDC and NHS. According to the PAMA: PβAE weight ratios (0:1, 1:1, 2:1, and 3:1), the samples were named PAMA 0, PAMA 50, PAMA 66, and PAMA 75, respectively.

PAMA/PβAE hydrogels were synthesized through a straightforward UV-initiated polymerization method. 10 wt% solutions of PAMA/PβAE in 1 mL of DCM were prepared and combined with a 1 wt% UV-initiator, DMPA. After vortexing for 60 s, the mixture was exposed to UV-A irradiation at a power density of 1.69 mW/cm^2 for 10 min. Once crosslinking occurred, the hydrogel was washed with 50 % ethanol for 15 min to eliminate any residual, unreacted initiator.

2.3. Material characterization

2.3.1. The physicochemical properties analysis

To study the chemical groups of PAMA/ PβAE, compared to PβAE, Fourier transform infrared spectra (FTIR, Tensor, Germany) were recorded using an FTIR spectrometer at 4000 and 400 cm^{-1}. The water vapor transmission rate (WVTR) was estimated based on the European Pharmacopoeia (EP) standard [26]. The samples with a diameter of 35 mm were positioned on the top of a bottle comprising 15 mL DDW. Subsequently, the bottles were incubated at 37 °C and a relative humidity of 35 %. Following a 24 h incubation period, the bottles were taken out and weighed again. The WVTR was determined using the Eq. (1) [27]:

$$\mathrm{WVTR}\left(\frac{g}{m^2}\right) = \frac{W_i - W_f}{A} \quad (1)$$

where W_i and W_f are the primary and ultimate weights of bottles, respectively, and A is the permeation surface of samples.

2.3.2. Adhesive strength evaluation

A shear assay was performed using cow's skin, by ASTM F2458–05 standards, to measure the adhesive properties of the PAMA/PβAE [28]. Briefly, cow skin was cut into small squares with a surface area of 1 cm^2. Two pieces of sheet metal were glued to the outer surfaces of the hair-removed skin. On the interior surfaces of both skin pieces, 100 μL of PAMA/PβAE solution containing 1 wt% DMPA was applied and exposed to UV radiation for 10 min. Finally, the samples were elongated at 1 mm/min until the separation. Stress-strain curves were used to establish the adhesive strength of PAMA/PβAE hydrogels.

2.3.3. L-Arginine release assay

The L-Arg concentration of PAMA/PβAE copolymers and L-Arg release from PAMA/PβAE hydrogels were investigated using the Bradford protein assay kit (Partocib, Iran). To evaluate L-Arg concentration,

the hydrogels were first cut into 1 × 1 cm^2, placed into 10 mL of PBS, and shaken at 150 rpm at 37 °C. Moreover, to measure L-Arg release, the different hydrogels were incubated in 10 mL of PBS solution at pH 5.6 and 7.4 ($n = 3$) for 14 days at 37 °C. At the specific times, 10 μL of PBS was transferred to a well and diluted with 80 μL of water. Next, 20 μL of reagent A, comprising Coomassie brilliant blue G-250 dye, was introduced into the wells and incubated for 5 min, facilitating the reaction with the L-Arg peptide. Lastly, the absorbance of the solutions was assessed at 595 nm using the microplate reader [29,30]. To determine the L-Arg content, a standard curve of BSA was prepared according to the manufacturer's protocol.

2.4. In vitro biological assay

2.4.1. Cell viability and morphology

Three types of cell lines, namely L929 fibroblasts, RAW-264.7 macrophages, and human umbilical vein endothelial cells (HUVECs), were acquired from the Iran National Cell Bank to examine the influence of PAMA on cellular interactions. Disc-shaped samples with a diameter of 10 mm ($n = 3$) were subjected to a 30-min immersion in 75 % ethanol and subsequently sterilized under UV light for 1 h. Next, cells at a density of 10^4 cells/well were seeded onto the samples, with a tissue culture plate (TCP) serving as the control group. The seeded cells were incubated in DMEM supplemented with 10 % FBS and 1 % streptomycin/penicillin for 5 days at 37 °C and 5 % CO_2. Following the incubation period, the cell viability and morphology were examined.

The cell viability was assessed using the MTT assay, according to the manufacturer's protocol (Sigma). At the end of 1, 3, and 5 days, the medium was removed, and 100 μL of MTT solution (5 mg/mL) was added to both the cell-seeded samples and the control group. The samples were then incubated for 4 h. Following the dissolution of the formazan crystals in DMSO, the optical density (OD) was measured using a microplate reader from BioRad (USA) at a wavelength of 490 nm, with DMSO as the reference. The relative cell survival was determined using Eq. (2) [31]:

$$\text{Relative cell survival (\%control)} = \frac{X_S - X_d}{X_t - X_d} \times 100 \quad (2)$$

where X_S, X_d, and X_t are OD values of the sample, DMSO (blank), and TCP (control), respectively.

The attachment and morphology of L929 cells were studied using Phalloidin/ DAPI staining. After 1, 3, and 5 days of culture, each cell-seeded sample was rinsed with PBS, fixed with 150 μL of 3.7 % PFA for 30 min, permeabilized with 0.1 % Triton X100 in PBS, and stained with Phalloidin and 1 % BSA and DAPI, respectively. The fluorescent microscopic images of samples were taken using a Nikon (Eclipse Ti, Japan) fluorescence microscope. Moreover, the cell density (cells/mm^2) of each sample was evaluated by ImageJ Software (2019).

2.4.2. Cell migration (scratch assay)

L929 fibroblast cells (3 × 10^4 cells/well) were seeded into 24 well plates as a model system and incubated for 24 h to provide a cell monolayer. According to previous studies [32], an *in vitro* wound healing assay was done using a 100 μL sterile pipette tip on the middle of the confluent surface and the hydrogels with a diameter of 10 mm, placed on both sides of the scratch and confluence cells surface. *In vitro* wound closure was imaged by an inverted microscope (Olympus, Japan) during 0, 12, and 24 h. Also, the cell-seeded TCP was used as the control. After 24 h, the wound closure was evaluated by ImageJ Software (2019, MRI wound healing tool).

2.4.3. Collagen deposition

To assess the expression level of the collagen I gene, L929 fibroblast cells at a density of 10^5 cells/mL were seeded on hydrogels in a 12-well plate and cultured for 24 and 48 h. At each time point, total RNA was extracted using an RNA extraction kit for subsequent real-time polymerase chain reaction (PCR) analysis. The concentration and purity of the extracted RNA were measured using a spectrophotometer (Nanodrop 100; Thermo Fisher Scientific, MA). Subsequently, cDNA synthesis was performed using a cDNA Synthesis Kit, starting with 1 mg of RNA. Real-time PCR was conducted using a SYBR Green PCR kit and controlled on a Bio-Rad real-time PCR system (Hercules, CA). Beta 2 Microglobulin (B2M) was used as the reference gene to normalize the expression levels of RNA. The primer sequences used are presented in Table 1. The DNA amplification process followed these conditions: 3 min at 95 ± 3 °C, 40 cycles of 10 s at 95 ± 3 °C and 30 s at 60 ± 2 °C, 1 min at 95 ± 3 °C, 1 min at 55 ± 2 °C, and 81 cycles of 10 s at 55 ± 2 °C. The amplification efficiency of the collagen I gene was determined relative to B2M ($\Delta Ct = Ct_{gene} - Ct_{B2M}$). The mRNA levels in each sample were calculated using the comparative ($\Delta\Delta Ct = \Delta Ct_{gene} - \Delta Ct_{control}$) method, and the relative expression of collagen I was determined using the formula $2^{-\Delta\Delta Ct}$ [33].

2.4.4. NO production

To evaluate the production of nitric oxide (NO), mouse RAW-264.7 macrophages at a density of 10^5 cells/mL were cultured on hydrogels in a 48-well plate, with TCP serving as the control group. Following 24 and 48 h of incubation, NO production was determined using the Griess reagent system. In this regard, 50 μL of the supernatant from each sample was added to 50 μL of 0.1 % N-1-naphthylethylenediamine dihydrochloride (NED) solution and 50 μL of sulfanilamide solution (1 % sulfanilamide in 5 % phosphoric acid). After 10-min incubation at room temperature, the absorbance of the solution at 540 nm was determined using the microplate reader. The amount of NO production was assessed by referring to a nitrite standard reference curve [14].

2.4.5. Inflammatory responses

To evaluate the inflammation factor, the disc-shaped hydrogels with 10 mm diameter ($n = 3$) were prepared, and the RAW-264.7 macrophages (10^6 cells/well) were seeded on samples for 24 h, followed by stimulation with 100 ng/mL LPS from *Escherichia coli* for 24 h [34]. The control 1 group (without LPS stimulation) and control 2 (with LPS stimulation) were similarly provided. Finally, an ELISA assay was performed to determine the cytokine level in the collected medium. ELISA kits were used to determine TNF-α, IL-6, IL-10, and TGF-β levels [35].

2.4.6. In vitro angiogenesis

A Matrigel-based model was used to evaluate the angiogenesis of HUVECs in contact with samples. In this regard, trypsinized HUVECs (10^5 cells/well) at passage 5 were seeded onto Matrigel, and 200 mL of each hydrogel extract was added. Following 24 h incubation, the tube formation was detected using an inverted microscope (Olympus, Japan). The tube length was considered using Image J software (Fiji vessel analysis tool) [36].

2.5. In vivo animal study

2.5.1. Surgical procedure

The animal experiments conducted in this study followed the standards accepted by the Animal Use and Care Administrative Advisory Committee of Isfahan University of Medical Sciences (ethical code # IR.MUI.AEC.1402.004). For wound closure evaluation, Sprague-Dawley (SD) rats (male, 16 weeks old, 250 g) were randomly divided into control (untreated wound), Commercial (Tegaderm™, M Health Care) and

Table 1
Specific Primers for Real-time PCR.

Gene	Primer sequence (forward)	Primer sequence (reverse)
Col I	AATTAATCTCAACAAACC	ATTTTTTGTGGTTGGGGAG
B2M	CCACTGAAAAAGATGAGTATGCCT	CCAATCCAAATGCGGCATCTTCA

optimized PAMA/PβAE hydrogel, according to *in vitro* experiments. First, disc-shaped samples with a diameter of 10 mm were sterilized under UV light for 1 h. Then, rats were anesthetized, shaved, and disinfected with iodine. A full-thickness square wound (diameter: 1 cm) was formed on the back of rats, followed by covering the defect sites with corresponding hydrogel. Next, the wounds were evaluated, according to the following experiments.

2.5.2. Wound healing evaluation

The wound was photographed at special time points (0, 7, and 14 days), and the surface area (A_0 and A_t) was estimated using Image J software. Based on the Eq. (3), the wound healing rate was calculated [37]:

$$\text{Wound healing rate } (\%) = \frac{A_0 - A_t}{A_0} \times 100 \quad (3)$$

After 14 days, the dorsal tissue was apart from the wound recovery area. Following fixation in 4 % PFA, it was embedded in paraffin and sectioned into 5-μm sections. Haemotoxylin and Eosin (H&E) staining was performed following the manufacturer's instructions (Sigma-Aldrich, USA) to study angiogenesis, granulation tissue formation, and epithelialization.

2.6. Statistical analysis

Statistical analysis of the data was done by the ANOVA test. To determine the significant difference between groups, the Tukey-Kramer *post hoc* test was applied using GraphPad Prism Software (Version 9). A p-value <0.05 was considered statistically significant.

3. Results and discussion

3.1. Physiochemical characterization of PAMA/PβAE

This study introduces a novel immunomodulatory wound dressing adhesive based on PAMA/PβAE for chronic wound healing. As shown in Fig. 1A, PAMA/PβAE hydrogels with various PAMA/PβAE weight ratios were prepared *via* a three-step process for chronic wound healing application by releasing nitric oxide (NO) and L-Arg at the wound site. Fig. 1B shows the L-Arg concentration in PAMA/PβAE copolymers. It was found that L-Arg loading efficiency was in the range of 55–79 %, depending on the copolymer composition. PAMA 50 wt% had significantly higher L-Arg loading efficiency between various samples, which could be related to the chemical interaction between PAMA and PβAE. The FTIR spectra of PAMA/PβAE copolymers, compared to PβAE, are presented in Fig. S1, supporting information. The spectrum of PβAE consisted of the prominent characteristic peaks at 1191 cm^{-1} (C—O), 1722 cm^{-1}(C═O stretching), 2962 cm^{-1} (methyl), 3421 cm^{-1} (N—H bonds), respectively, confirming PβAE was successfully synthesized [38]. Compared to PβAE, the spectra of the copolymers were noticeably different. In this spectrum, new peaks at 2700 cm^{-1} (CH), 1188 cm^{-1} (C—O), and 3390 cm^{-1} (N—H) were detected due to copolymerization of polymers by using EDC/NHS [39]. The water vapor permeability rate of skin wound dressing is one of the principal properties of wound dressings [40]. For ideal wound dressing, the WVTR should be 2000-2500 g/m^2 to prevent dryness and loss of water and exudate formation in the wound bed [41]. As shown in Fig. 1C, the WVTR of PAMA/PβAE hydrogels was 1760–2080 g/m^2. In addition, water vapor permeability was enhanced with increasing PAMA content. Similarly, Zhang et al. [42] found that increasing L-Arg content in the dopamine-hyaluronic acid hydrogels resulted in the formation of porous structures and enhanced water vapor permeability rate. Accordingly, our results demonstrated that PAMA 66 and PAMA 75 could have the potential for wound dressings.

3.2. Ex vivo adhesive properties of PAMA/PβAE

To assess the suitability of PAMA/PβAE as a wound dressing, the adhesive strength of the hydrogels was measured using cow skin (Fig. 2A). Fig. 2B shows the adhesive strength of PAMA/PβAE hydrogels, compared with Evicel and Coseal commercial wound dressings [43]. Results revealed that the adhesive strength of PAMA/ PβAE hydrogels in the range of 25–43 kPa was significantly higher than both commercial wound dressings. The adhesion strength is a combination of adhesive and cohesive strengths, and a balance between them is critical to provide an appropriate adhesion [44]. The suitable adhesive strength characteristics of the PAMA/ PβAE hydrogels could be related to hydrogel-tissue interlocking [45], hydrogen bonding between free hydroxyl and amine groups [46], and chemical bonding with radicals created during the crosslinking process [47].

3.3. The release of L-arginine from PAMA/PβAE

According to our knowledge, L-Arg has a double-edged sword role in the wound-healing process [48]. Hence, L-Arg content should be controlled *via* polymerization PAMA and copolymerization with PβAE to facilitate healing and reduce nonfunctional scarring. Therefore, we examined L-Arg release from PAMA/PβAE hydrogels in phosphate buffer at pH 5.6 and pH 7.4 for 14 days. As shown in Fig. 2C and D, L-Arg were released from hydrogels at various rates, depending on the pH value of the environment. Interestingly, the L-Arg release rate of hydrogels increased (between 35 and 57 %) at pH 5.6 compared to pH 7.4 (between 20 and 34 %) during 5 days, according to the pH sensitivity of PAMA/PβAE hydrogels. As shown in Fig. 2C, D, owing to various PAMA concentrations, the L-Arg release was different among the hydrogels over 14 days. Particularly, during the first 7 days, the released L-Arg from PAMA 66 wt% and 75 wt% were higher than that of PAMA 50 wt%, confirming a superior local concentration of L-Arg at the wound area. Similarly, Ling et al. [12] evaluated the release of L-Arg from bioactive chitosan/L-Arg hydrogels. Their study demonstrated that a high concentration of L-Arg promoted skin repair with minus scar formation by faster L-Arg release kinetics during the first 9 days. The L-Arg release process from PAMA/PβAE hydrogels was started with hydrolysis leading to amide bond cleavage between L-Arg and PβAE. This unique L-Arg release profile, initiated with accumulative release followed by sustained release kinetic, could be suitable for wound healing, resulting in suitable wound repair with sufficient collagen deposition and a controlled immunomodulatory response [12,49].

3.4. Fibroblast responses mediated by PAMA/PβAE hydrogels

To investigate the potential of PAMA/PβAE hydrogels for wound healing, the interaction of various cell lines such as fibroblasts (L-929), endothelial (HUVEC), and macrophage (RAW-264.7) cells, with hydrogels was examined. First, a straightforward approach was taken to determine the potential toxicity of hydrogels by MTT assay. As shown in Fig. 3A, L929 cells maintained a rapid growth rate with increasing culture time in contact with all samples without obvious cytotoxicity. The viability of L929 cells enhanced with increasing PAMA content at the PAMA 66. It might be due to more L-Arg resulting in higher cell viability during 5 days. Moreover, the morphology of L929 cells stained with DAPI/Phalloidin was investigated after 1, 3, and 5 days of culture (Fig. 3B). Results showed that L929 cells adhered and grew well on the surface of all hydrogels. After the first day of culture, the cells started elongating and spreading, depending on the sample types. Noticeably, as shown in Fig. 3C, cell spreading on PAMA 66 and PAMA 75 (280 cells/mm^2) was significantly higher than the two other samples (PAMA 0 and PAMA 50), indicating the effective role of PAMA in improving cell attachment and spreading. It could be due to the increasing amount of L-Arg and NO release by increasing PAMA content, accelerating cell proliferation and enhancing attachment.

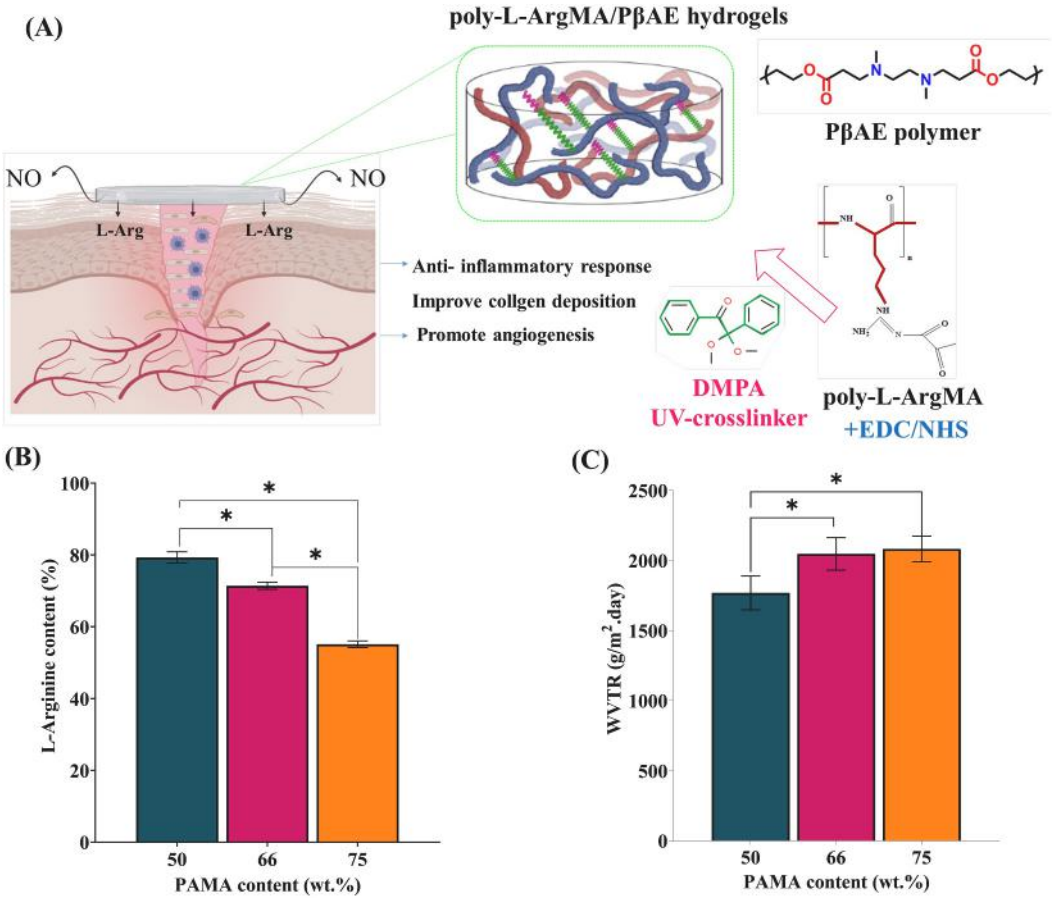

Fig. 1. A) The schematic illustration of the design of a suitable wound dressing such as PAMA/ PβAE hydrogels with desired angiogenesis, anti-inflammatory response, collagen deposition, and cell proliferation. B) L-Arg content of different PAMA/ PβAE hydrogels. C) WVTR of PAMA/ PβAE hydrogels with different PAMA contents. The results are reported as the means ($n = 3$) ± standard deviation (*: $P < 0.05$).

A scratch wound-healing assay was performed to examine the potential of PAMA/PβAE hydrogels to stimulate cell migration. As shown in Fig. 4A, B, PAMA/PβAE considerably diminished the wound gap in a time-dependent manner. The PAMA 66 and PAMA 75 treatments resulted in 50 % increased cell migration during 12 h and 24 h compared to the control group. Moreover, collagen type I gene expression (Fig. 4C) measured in L929s also demonstrated that all PAMA-content samples revealed a higher expression of collagen type I than the control group. Between them, PAMA 66 showed the most increased collagen I expression, possibly due to the higher cumulative L-Arg release stimulating the proliferation and migration of skin cells. Similarly, Hussein et al. [50] revealed improved fibroblast migration in contact with PVA/hyaluronic acid/L-Arg nanofibrous scaffolds due to the release of L-Arg. Improved formation and maturation of granulation tissue at the wound site could lead to the development of an ECM for re-epithelialization and blood vessel sprouting. It could benefit the early stages of wound healing [51]. By increasing PAMA in hydrogel structure, more L-Arg was released early, promoting collagen production. It has been noted that fibroblasts derived from wounds have the ability to increase the expression of arginase. This enzyme facilitates the conversion of L-Arginine into ornithine, which serves as a precursor for proline production. Proline, in turn, acts as a crucial substrate material for the collagen synthesis [52]. Similarly, Ling et al. [12] evaluated the role of chitosan/L-Arg hydrogels in collagen I and III depositions. It showed that controlling L-Arg release could promote collagen synthesis in the early wound healing process with less scar formation in a rat model. In summary, it could be found that PAMA/PβAE hydrogels could facilitate collagen type I synthesis, which may enhance immunomodulatory parameters during wound healing.

3.5. Inflammation responses mediated by PAMA/PβAE hydrogels

Macrophages are responsible for various steps of wound healing, such as inflammation and remodeling phases. First, a straightforward approach was taken to determine the potential toxicity of hydrogels by MTT assay. As shown in Fig. 5A, the PAMA/PβAE hydrogels supported RAW macrophage survival and growth, indicating their cytocompatibility. However, enhanced cell viability was found in each group with the prolongation of culture time. Intriguingly, PAMA 50 and PAMA 66 groups displayed higher cell viability than other hydrogel and control, proposing its noble potential in immune cell responses. Intriguingly, PAMA 50 and PAMA 66 hydrogels showed better RAW cell viability than PAMA 75, implying that they might be helpful for skin tissue engineering.

Various copolymer samples investigated the potential for inducing NO production, pro-inflammatory, and anti-inflammatory cytokines in RAW-264.7 macrophages. As shown in Fig. 5B, macrophages responded immediately to samples, and the generated NO, depending on the PAMA content. After 24 h incubation, NO release enhanced from 4.06 ± 0.6 μM to 8.21 ± 0.9 μM when the PAMA content changed from 50 wt% to 66 wt% (Fig. 5B). These values were more significant than the control group (0.46 ± 0.1 μM). Our results supported previous evidence of enhanced L-Arg release by increasing the PAMA content from 66 wt% to 75 wt%. It is well-known that macrophages can metabolize L-Arg *via* two mechanisms, comprising NO production and ornithine for collagen synthesis [53]. In the early stages of wound healing, the microenvironment induces iNOS expression, attracting activated macrophages (M1 macrophages) to the wound site. L-Arg also serves as the sole substrate for NO production by iNOS. NO is widely recognized as a potent

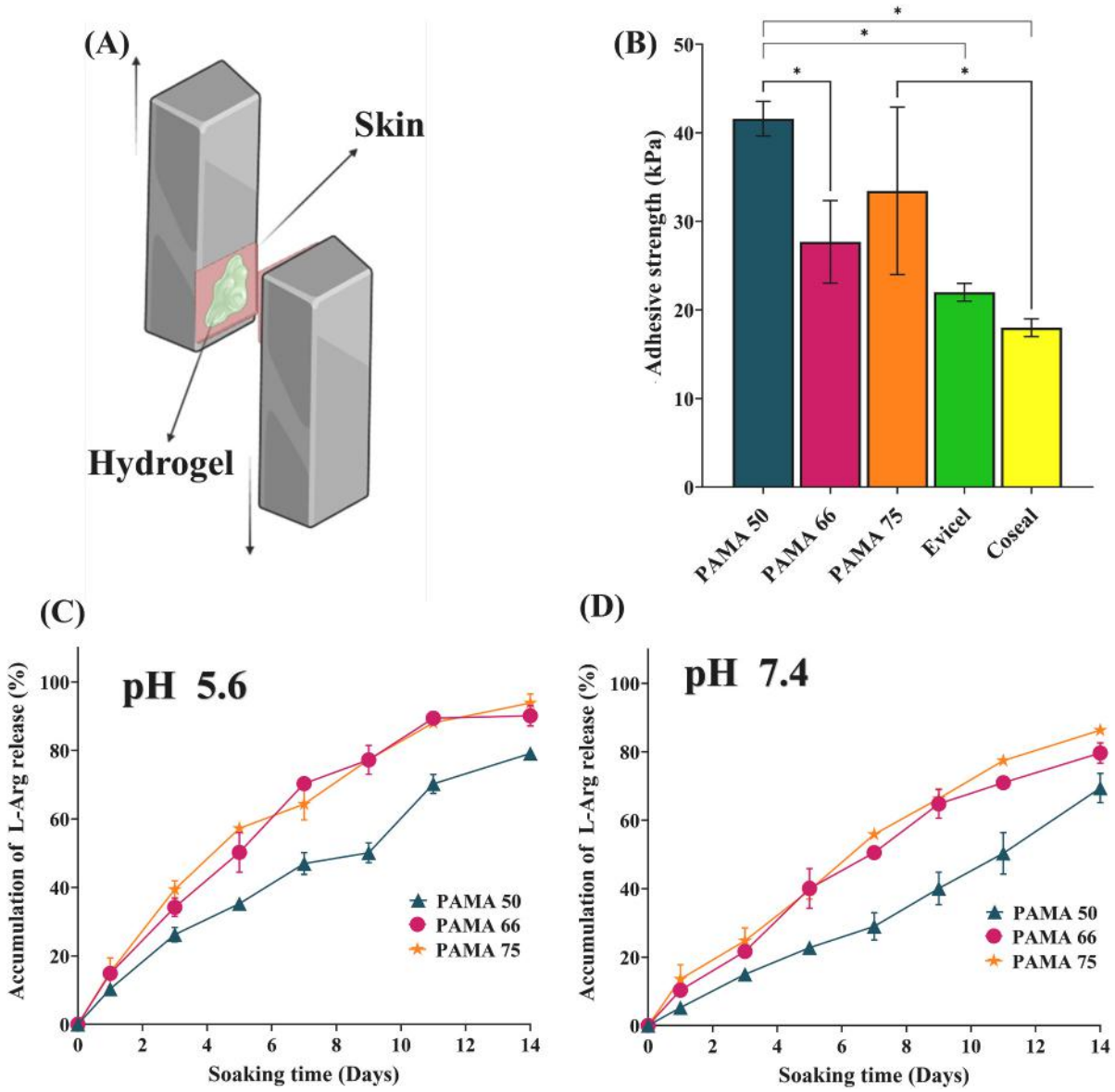

Fig. 2. Physiochemical properties of PAMA/ PβAE hydrogels: A) The schematic of the adhesive strength evaluation system and B) the average adhesive strength of different PAMA/ PβAE hydrogels. *In vitro* L-Arg cumulative release of PAMA/ PβAE hydrogels incubated in PBS for 14 days C) at pH 5.6, and D) at pH 7.4. The results are reported as the means ($n = 3$) ± standard deviation (*: $P < 0.05$).

immunomodulatory factor produced by macrophages. It plays a crucial role in promoting wound healing through diverse mechanisms, such as inhibiting infections, increasing angiogenesis, and facilitating re-epithelialization [54]. Additionally, PAMA/PβAE hydrogel was characterized by the expression of pro-inflammatory (IL-6, and TNF-α) and anti-inflammatory (IL-10, and TGF-β) markers. Compared to untreated cells, the macrophages treated with PAMA/PβAE and LPS showed higher IL-10 and TGF-β and lower levels of IL-6 and TNF-α (Figs. 5 C—F). Moreover, between samples, PAMA 66 significantly increased the expression of anti-inflammatory markers (Fig. 5E and F) while reducing the expression of pro-inflammatory markers (Fig. 5C and E). Similarly, He et al. [55] studied the immunomodulation properties of L-Arg-based poly(ester amine) copolymer for chronic skin wound healing. Our results confirmed that L-Arg-based PβAE copolymer with higher L-Arg content and tunable NO production (~9 μM) resulted in an increased TGF-β1 expression and decreased TNF-α, which might modulate the phenotypes of various cells and contribute to the transition from the pro-inflammatory stage to the anti-inflammatory stage at the site of the wound. However, this study showed that the IL-10 and TGF-β markers were significantly elevated and the IL-6 and TNF-α opposite tendency with remarkably decreased levels using PAMA/PβAE hydrogels (Fig. 5C-F). As shown in Fig. 6G, all results demonstrated that PAMA/PβAE hydrogels could effectively activate macrophage polarization to M2 phenotype, control inflammation responses, and promote the vascularization and the expression of collagen.

3.6. *In vitro* angiogenesis

One of the most abundant cells in the wound tissue is endothelial cells (HUVECs), which are responsible for wound healing. First, a straightforward approach was taken to determine the potential toxicity of hydrogels by MTT assay. As shown in Fig. 6A, HUVECs maintained a rapid growth rate with increasing culture time in contact with all samples without obvious cytotoxicity. In addition, the PAMA 75 group revealed slightly lower HUVEC viability than other groups after 5 days. Therefore, an excessive presence of PAMA within the hydrogels could have an adverse effect on the viability of HUVECs. Intriguingly, PAMA 50 and PAMA 66 hydrogels improved HUVEC viability than PAMA 75,

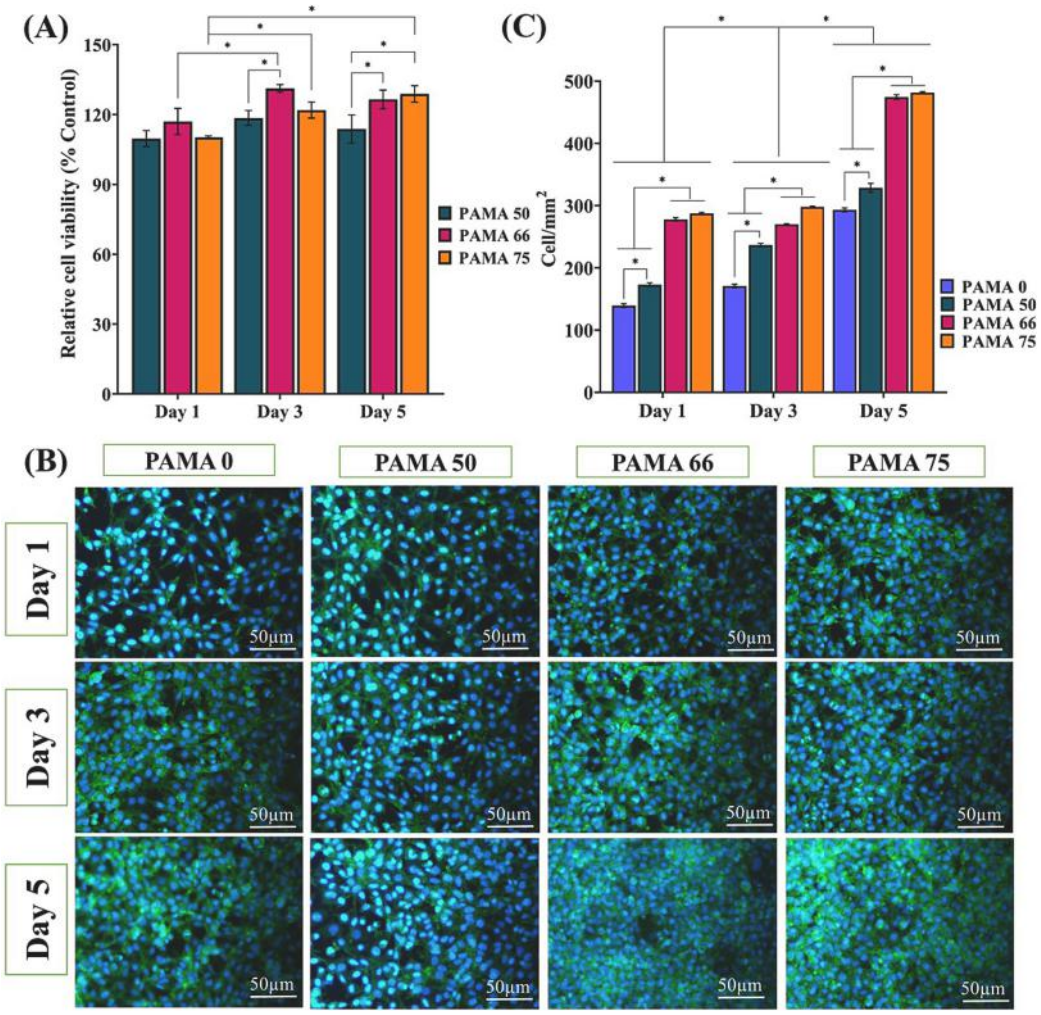

Fig. 3. Fibroblast cell responses to PAMA/PβAE hydrogels: A) The relative cell viability in contact with PAMA/PβAE hydrogels, evaluated using the MTT assay over 5 days. The obtained results were normalized against the control group (TCP). B) CLSM images of L929 cells cultured on the PβAE and PAMA/PβAE for 1, 3, and 5 days. C) The density of L929 cells/ mm^2 of hydrogels during the 5 days of culture. The results are reported as the means ($n = 3$) ± standard deviation (*: $P < 0.05$).

suggesting that they might be helpful for skin tissue engineering.

The angiogenesis activity of PβAE and PAMA/PβAE hydrogels was further studied *in vitro* using the tube-formation ability of HUVECs. As shown in Fig. 6B-E, treatment of HUVECs with PAMA/PβAE extracts resulted in the development of a well-defined tubular network, which could potentially be attributed to the production of NO induced by L-Arg in the endothelial cells. Earlier studies have shown that endothelial cells can metabolize L-Arg available in the medium through the action of NOS, resulting in the production of NO, which in turn promotes angiogenesis [56]. Furthermore, PAMA/PβAE samples formed comparable and even better tubular networks than PβAE, which might be due to the effect of PAMA. It was consistent with other studies on the L-Arg effect [57]. The quantitative analysis revealed that the average total tube length of copolymers was ~84,000 and 87000px, higher than PAMA 0 (75000px) and the control group (71000px). Similarly, Ling et al. [14] evaluated the angiogenesis properties of bioactive chitosan/L-Arg hydrogels and demonstrated that this hydrogel could promote angiogenesis through sustained NO production at the wound site and control immunomodulatory activity. According to previous studies, L-Arg released from PAMA/PβAE could stimulate angiogenesis since L-Arg can be converted into NO, which supports endothelial cell proliferation by upregulating the expression of vascular endothelial growth factor (VEGF) and βFGF and migration [58]. In summary, the PAMA/PβAE hydrogels, with varying PAMA content but similar angiogenic properties, have the potential to promote angiogenesis at the wound site, ultimately leading to improved wound healing.

3.7. *In vivo wound healing enhanced by PAMA/PβAE*

According to our results, the PAMA 66 with suitable mechanical properties, biocompatibility, the best collagen I expression, and ideal immunomodulatory responses and angiogenesis were selected for *in vivo* studies. To develop an *in vivo* wound healing model, a full-thickness wound defect (1 × 1 cm^2) was created in a rat model (Fig. 7A). At the specified intervals of time (0, 7, and 14 days), the wound healing ratio after treatment with PAMA 66 hydrogel, commercial wound dressing (Tegaderm™), and without any treatment (as a control group) was determined. As shown in Fig. 7B, compared to the control (~37 %) and commercial dressing (~52 %), the PAMA 66 sample improved wound repair by approximately 65 % after 7 days of treatment. Significant progress in wound healing was particularly noticeable on the 14th day when the PAMA 66 hydrogel exhibited a remarkable wound healing ratio of approximately 98 % and demonstrated the swiftest rate of wound contraction compared to the control (~62 %) and Tegaderm™ (~80 %). The data might be related to the NO production and L-Arg sustained release at the wound site. For example, in the study conducted by Ling et al. [12], the efficiency of chitosan/L-Arg hydrogel in promoting wound healing was assessed. The *in vivo* findings signified that applying L-Arg/chitosan hydrogel on rat models resulted in significant improvements, with approximately 98 % of the wounds being closed by

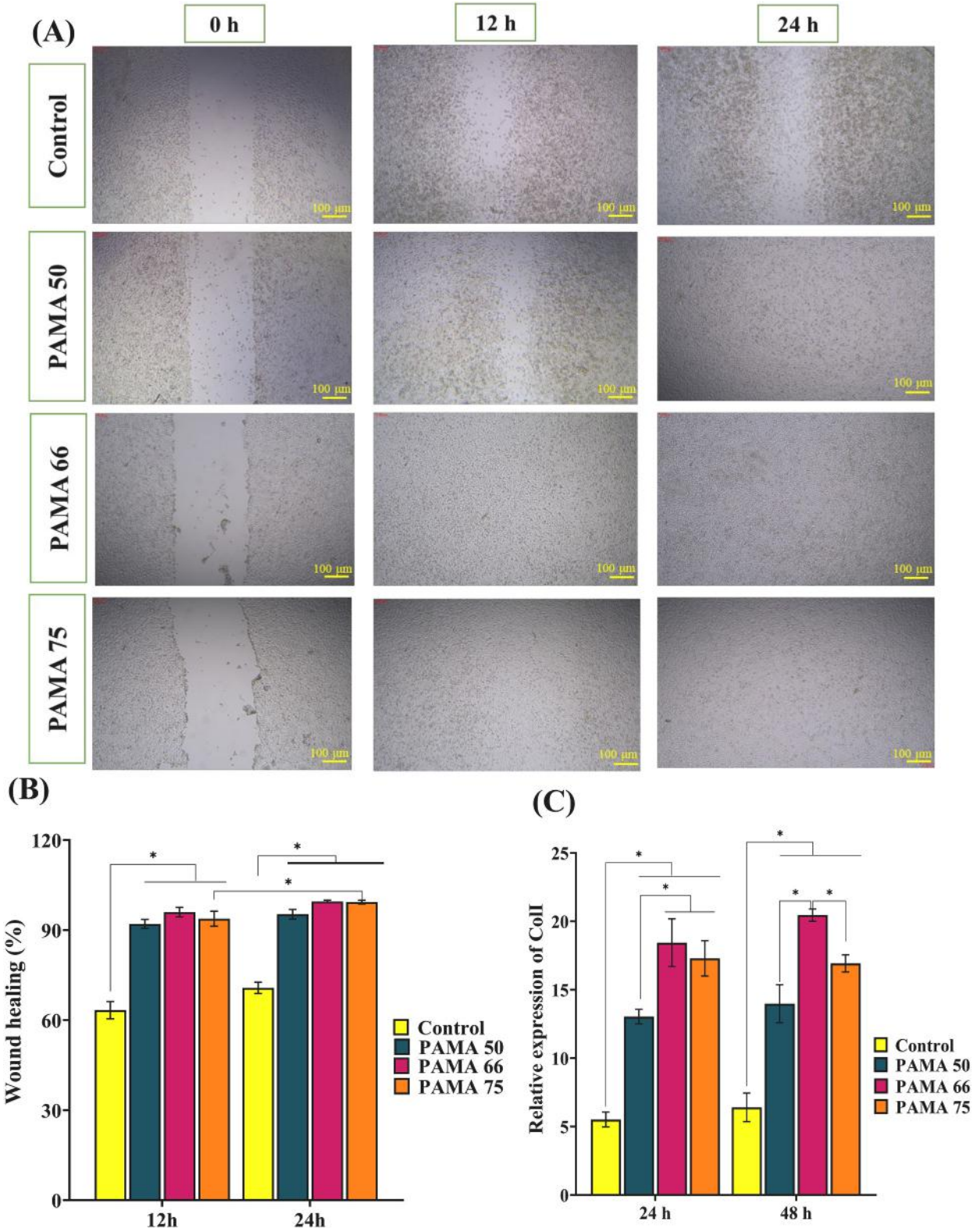

Fig. 4. Fibroblast cells responses to PAMA/PβAE hydrogels: A) The scratch wound assay images and B) its analysis on L929 treated with PAMA/ PβAE hydrogels for 12 h and 24 h. C) The real-time PCR analysis of collagen I expression of L929 cells after being treated with PAMA/PβAE hydrogels during 24 h and 48 h. The untreated cells were the control group. The results are reported as the means ($n = 3$) ± standard deviation (*: $P < 0.05$).

day 14. In comparison, the control group exhibited only around 79 % wound closure. Moreover, Zhao et al. [59] evaluated a wound-healing process with Arg-modified chitosan-oligosaccharide (COS-Arg)-doped hydrogel and demonstrated that by adding Arg to the hydrogel system the wound-healing ratio promoted and reduced inflammatory responses.

The H&E staining assay of wound skin was done to understand the underlying mechanism for improved wound healing treated with PAMA 66 hydrogel. Fig. 7C demonstrated that during 14 days post-treatment,

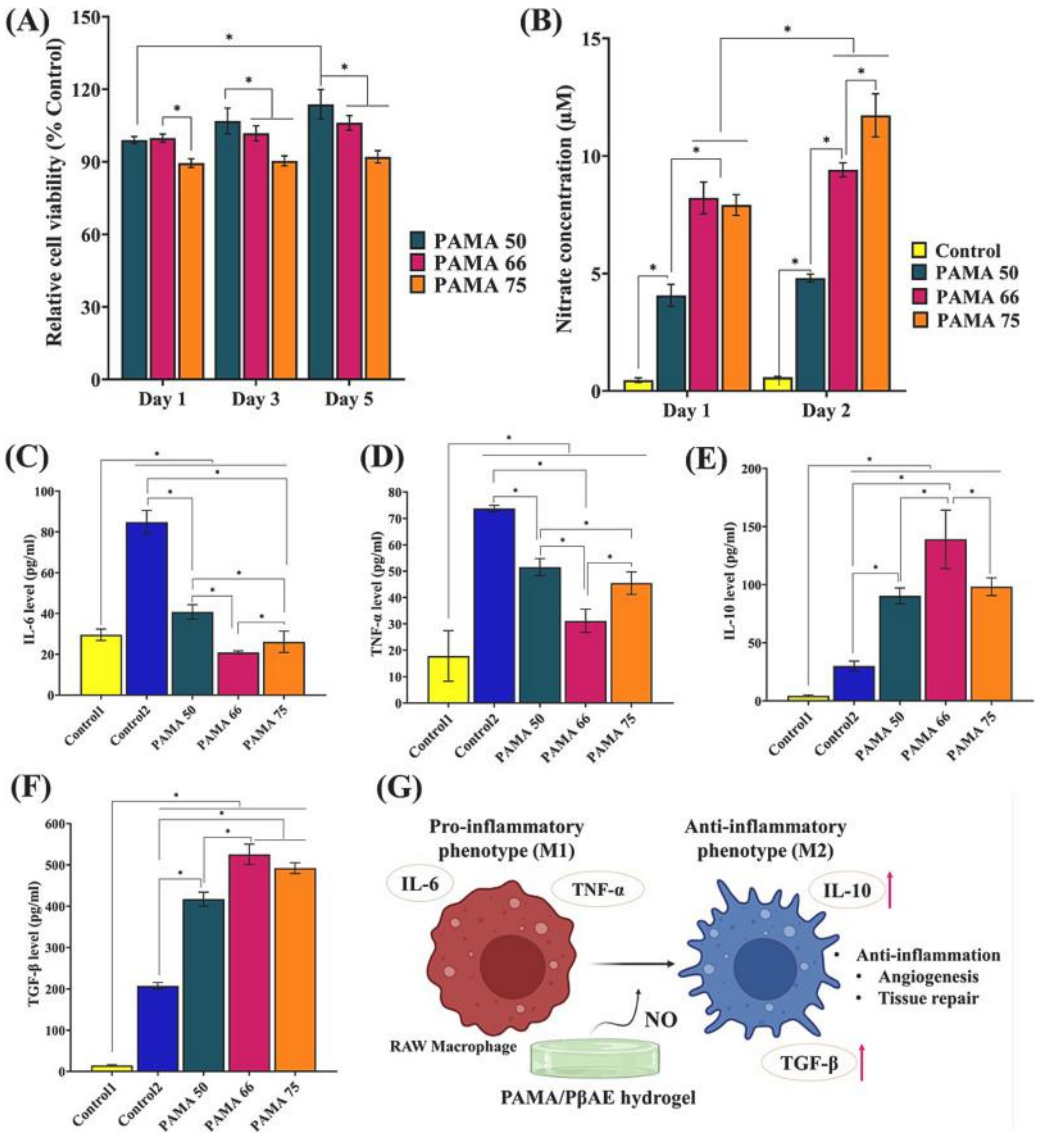

Fig. 5. Macrophage cell responses to PAMA/PβAE hydrogels: A) Relative cell viability in contact with PAMA/PβAE hydrogels estimated using the MTT test. The results are normalized against the control (TCP). B) *In vitro* NO production by RAW-264.7 macrophage during 24 h and 48 h. ELISA analysis of macrophage cytokines including C) IL-6, D) TNF-α, E) IL-10, F) TGF-β after 48 h. The untreated cells without LPS and with LPS were used as the control 1 and control 2 groups, respectively. The results are reported as the means ($n = 3$) ± standard deviation (*: $P < 0.05$). G) The schematic representing macrophage phenotypes in interaction with PAMA/PβAE.

more epidermis thickness (~2 times), dermis thickness (~1.6 times), vascularization (~3 times), and hair follicles (~2.5 times) were observed in PAMA 66 group compared to the control, that should be related to the contribution of L-Arg and NO interaction with skin cells (Fig. 7 D-G). Also, the damaged skin tissue repair indicators compared to Tegaderm™ as a commercial dressing demonstrated that in the PAMA 66 group epidermis thickness (~1.2 times), dermis thickness (~1.3 times), and vascularization (~1.5 Times) were improved during 14 days. Meanwhile, Tegaderm™, as well as PAMA 66 hydrogel, could enhance the formation of new hair follicles at repaired skin tissue.

Blood vascularization, which promotes nutrition, oxygenation, and waste transfer, is essential for wound healing [60]. On day 7, the wounds treated with PAMA 66 hydrogel showed more fibroblast infiltration and more evident neovascularization than the control and commercial dressing, crucial for granulation maturity and wound contraction. Remarkably, on day 14, the blood vessel numbers increased slowly in PAMA 66 hydrogel, similar to other groups. The PAMA 66 groups effectively eliminated unmatured blood vessels, creating a favorable environment for subsequent phases of matrix remodeling. Furthermore, the PAMA 66 group exhibited greater growth in skin layers compared to the control and Tegaderm™ group, indicating the enhanced wound-healing capabilities of PAMA 66. Similarly, Zou et al. [60] created a tissue adhesive using a combination of L-Arg-based degradable polyurethane and gelatin methacrylate to expedite the process of wound healing. The *in vivo* findings demonstrated that the hydrogel adhesive had a notable impact, as it significantly increased the thickness of the dermis and improved vascularization by 2.5 times compared to the control.

The overall outcome of our study can be credited to the ability of the PAMA 66 wt% hydrogel to release L-Arg and NO, which encourage vascular endothelial and skin cell proliferation. This mechanism helps regulate immune responses and ultimately speeds up the process of tissue repair. It is highlighted that the PAMA 66 hydrogel is a promising wound dressing that can promote the chronic wound healing.

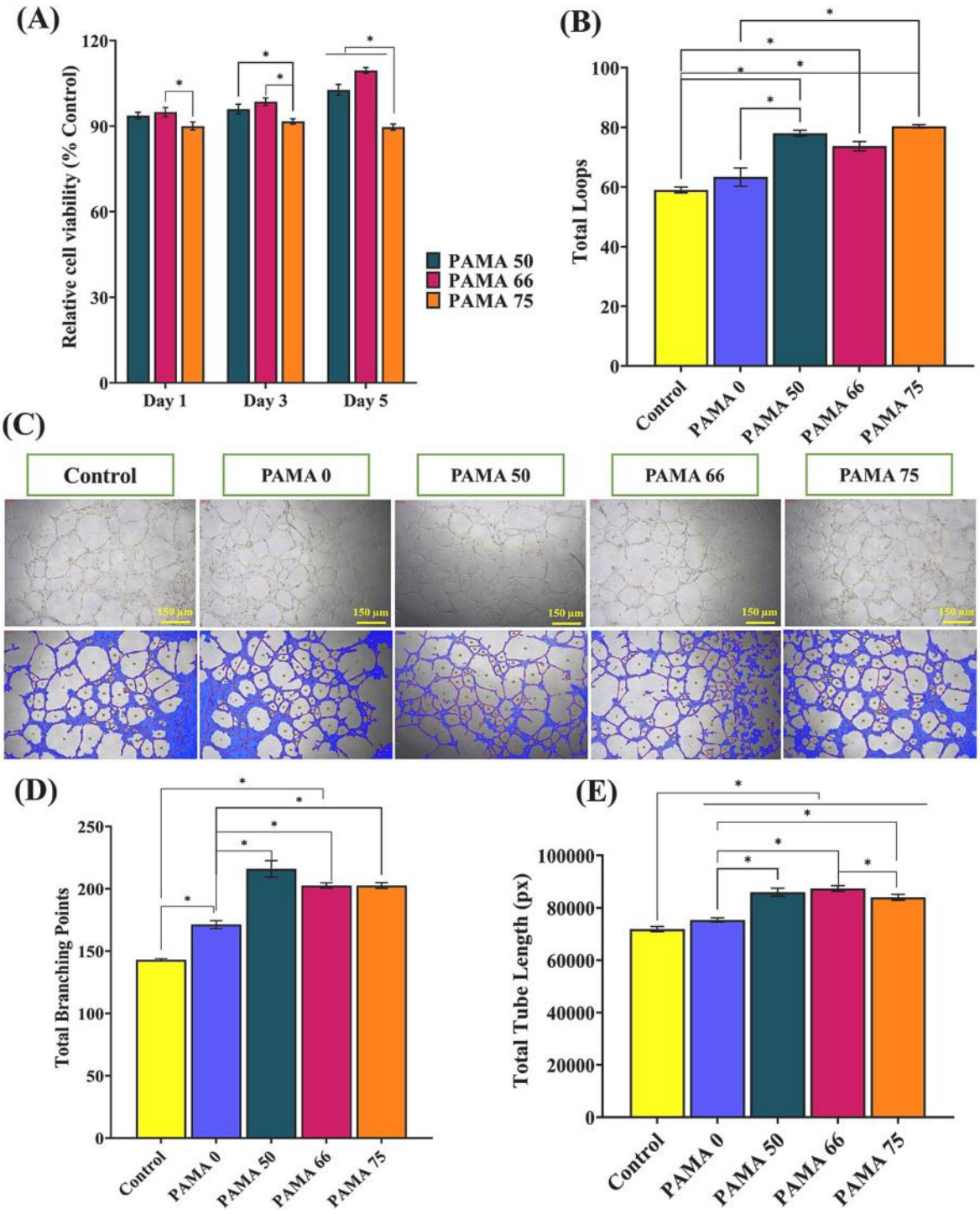

Fig. 6. Endothelial cell responses to PAMA/PβAE hydrogels: A) Relative cell viability in contact with PAMA/PβAE hydrogels determined using the MTT test for 5 days. The results are normalized against the control (TCP). *In vitro* angiogenesis assay prompted by PAMA/PβAE hydrogels for 24 h: B) Quantitative evaluation of total loops, C) digital images of tube formation by HUVECs, D) quantitative evaluation of total branching point, and E) total tube length. The untreated cells were used as the control group. The results are reported as the means ($n = 3$) ± standard deviation (*: $P < 0.05$).

4. Conclusion

In conclusion, we have effectively fabricated a novel immunomodulatory PAMA/PβAE hydrogel to promote chronic wound healing *via* NO production and sustained L-Arg release. Varying the PAMA content resulted in tunable adhesive strength, water vapor permeability, L-Arg release profiles, and cell responses. Interestingly, the PAMA 66 hydrogel exhibited remarkable functionality by enhancing the adhesion, proliferation, migration, and collagen I gene expression of L929 cells. It effectively activated macrophages to produce NO molecules and regulated the response of pro-inflammatory and anti-inflammatory immune cells. The PAMA/PβAE hydrogels also demonstrated their ability to promote angiogenesis in HUVECs, which can be related to the unique release profile of L-Arg from the hydrogels. Furthermore, *in vivo* experiments confirmed that the PAMA 66 hydrogel promoted angiogenesis and accelerated wound healing. Overall, the PAMA/PβAE hydrogel with

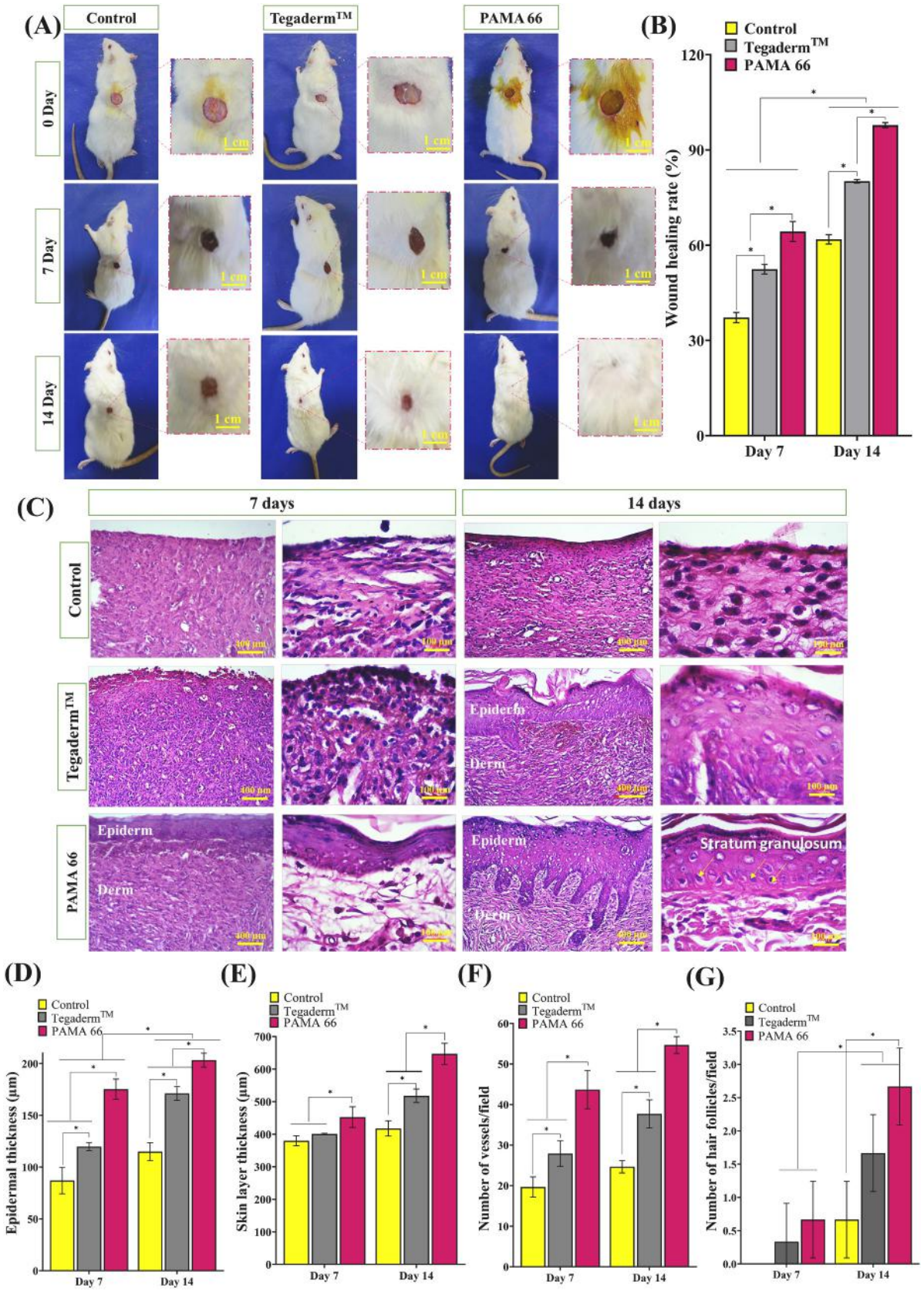

Fig. 7. *In vivo* wound healing study: A) Photographs showing PAMA/ PβAE hydrogel-treated wounds, compared to control (untreated wound) and commercial wound dressing (Tegaderm™) at 0, 7, and 14 days. B) Quantitative analysis of wound healing ratio (%). C) H&E staining histopathological evaluation of wound sections under various conditions. D) The average epidermis thickness, E) the average skin thickness, and F) the average blood vessels at 7- and 14 days post-treatment. G) Quantification of regenerated hair follicles following different treatments for 7 and 14 days. The results are reported as the means ($n = 3$) ± standard deviation (*: $P < 0.05$).

controlled release of L-Arg and NO production has great potential as an effective wound dressing for enhancing the healing of chronic skin wounds.

Supplementary data to this article can be found online at https://doi.org/10.1016/j.bioadv.2024.213762.

CRediT authorship contribution statement

Parisa Heydari: Formal analysis, Investigation, Software, Writing – original draft, Writing – review & editing. **Mahshid Kharaziha:** Methodology, Resources, Supervision, Writing – review & editing. **Jaleh Varshosaz:** Funding acquisition, Methodology, Supervision. **Anousheh Zargar Kharazi:** Funding acquisition. **Shaghayegh Haghjooy Javanmard:** Methodology, Writing – review & editing.

Declaration of competing interest

The authors declare that they have no known competing financial interests or personal relationships that could have appeared to influence the work reported in this paper.

Data availability

Data will be made available on request.

Acknowledgments

The authors gratefully thank the financial support provided by Isfahan University of Medical Sciences through grant No. # 1401335 and grant No. # 199090.

References

[1] L. Sheng, Z. Zhang, Y. Zhang, E. Wang, B. Ma, Q. Xu, L. Ma, M. Zhang, G. Pei, J. Chang, A novel "hot spring"-mimetic hydrogel with excellent angiogenic properties for chronic wound healing, Biomaterials 264 (2021) 120414.
[2] J. Chi, X. Zhang, C. Chen, C. Shao, Y. Zhao, Y. Wang, Antibacterial and angiogenic chitosan microneedle array patch for promoting wound healing, Bioact. Mater. 5 (2020) 253–259.
[3] J.S. Kim, H. Yu, M.R. Woo, D.W. Kim, J.O. Kim, S.K. Ku, S.G. Jin, H.-G. Choi, Influence of hydrophilic polymers on mechanical property and wound recovery of hybrid bilayer wound dressing system for delivering thermally unstable probiotic, Mater. Sci. Eng. C 112696 (2022).
[4] S. Ma, Y. Yang, Y. Mu, H. Peng, P. Wei, W. Jing, C. Peng, X. Liu, B. Zhao, M. Cai, Modification of the small intestinal submucosa membrane with oligopeptides screened from intrinsically disordered regions to promote angiogenesis and accelerate wound healing, Biomater. Adv. 148 (2023) 213360.
[5] M. Kharaziha, A. Baidya, N. Annabi, Rational design of immunomodulatory hydrogels for chronic wound healing, Adv. Mater. 33 (2021) 2100176.
[6] P. Heydari, M. Kharaziha, J. Varshosaz, S.H. Javanmard, Current knowledge of immunomodulation strategies for chronic skin wound repair, J. Biomed. Mater. Res. Part B Appl. Biomater. 110 (2021) 265–288.
[7] G.Q. Teixeira, C.L. Pereira, F. Castro, J.R. Ferreira, M. Gomez-Lazaro, P. Aguiar, M. A. Barbosa, C. Neidlinger-Wilke, R.M. Goncalves, Anti-inflammatory chitosan/poly-γ-glutamic acid nanoparticles control inflammation while remodeling extracellular matrix in degenerated intervertebral disc, Acta Biomater. 42 (2016) 168–179.
[8] K. Nuutila, M. Samandari, Y. Endo, Y. Zhang, J. Quint, T.A. Schmidt, A. Tamayol, I. Sinha, In vivo printing of growth factor-eluting adhesive scaffolds improves wound healing, Bioact. Mater. 8 (2022) 296–308.
[9] J. McMasters, A. Panitch, Collagen-binding nanoparticles for extracellular anti-inflammatory peptide delivery decrease platelet activation, promote endothelial migration, and suppress inflammation, Acta Biomater. 49 (2017) 78–88.
[10] H. Singh, S.M. Bashir, S.D. Purohit, R. Bhaskar, M.A. Rather, S.I. Ali, I. Yadav, M.U. D. Dar, M.A. Gani, M.K. Gupta, Nanoceria laden decellularized extracellular matrix-based curcumin releasing nanoemulgel system for full-thickness wound healing, Biomater. Adv. 137 (2022) 212806.
[11] R. Ahmed, R. Augustine, M. Chaudhry, U.A. Akhtar, A.A. Zahid, M. Tariq, M. Falahati, I.S. Ahmad, A. Hasan, Nitric oxide-releasing biomaterials for promoting wound healing in impaired diabetic wounds: state of the art and recent trends, Biomed. Pharmacother. 149 (2022) 112707.
[12] Z. Ling, J. Deng, Z. Zhang, H. Sui, W. Shi, B. Yuan, H. Lin, X. Yang, J. Cao, X. Zhu, Spatiotemporal manipulation of L-arginine release from bioactive hydrogels initiates rapid skin wound healing accompanied with repressed scar formation, Appl. Mater. Today 24 (2021) 101116.
[13] A.P. Ralph, P.M. Kelly, N.M. Anstey, L-arginine and vitamin D: novel adjunctive immunotherapies in tuberculosis, Trends Microbiol. 16 (2008) 336–344.
[14] Z. Ling, Z. Chen, J. Deng, Y. Wang, B. Yuan, X. Yang, H. Lin, J. Cao, X. Zhu, X. Zhang, A novel self-healing polydopamine-functionalized chitosan-arginine hydrogel with enhanced angiogenic and antibacterial activities for accelerating skin wound healing, Chem. Eng. J. 420 (2021) 130302.
[15] L. Jiang, K. Wang, L. Qiu, Doxorubicin hydrochloride and L-arginine co-loaded nanovesicle for drug resistance reversal stimulated by near-infrared light, Asian, J. Pharm. Sci. 17 (2022) 924–937.
[16] G. Mao, S. Tian, Y. Shi, J. Yang, H. Li, H. Tang, W. Yang, Preparation and evaluation of a novel alginate-arginine-zinc ion hydrogel film for skin wound healing, Carbohydr. Polym. 311 (2023) 120757.
[17] L. Zhou, H. Zheng, Z. Liu, S. Wang, Z. Liu, F. Chen, H. Zhang, J. Kong, F. Zhou, Q. Zhang, Conductive antibacterial hemostatic multifunctional scaffolds based on Ti3C2T x MXene nanosheets for promoting multidrug-resistant bacteria-infected wound healing, ACS Nano 15 (2021) 2468–2480.
[18] J.E. Park, M.J. Abrams, P.A. Efron, A. Barbul, Excessive nitric oxide impairs wound collagen accumulation, J. Surg. Res. 183 (2013) 487–492.
[19] J. Zhu, J. Tian, C. Yang, J. Chen, L. Wu, M. Fan, X. Cai, L-Arg-rich amphiphilic dendritic peptide as a versatile NO donor for NO/photodynamic synergistic treatment of bacterial infections and promoting wound healing, Small 17 (2021) 2101495.
[20] N. Sahiner, One step synthesis of an amino acid derived particles, poly (L-arginine) and its biomedical application, Polym. Adv. Technol. 33 (2022) 831–842.
[21] Z. Sun, X. Wang, J. Liu, Z. Wang, W. Wang, D. Kong, X. Leng, ICG/l-arginine encapsulated PLGA nanoparticle-thermosensitive hydrogel hybrid delivery system for cascade cancer photodynamic-NO therapy with promoted collagen depletion in tumor tissues, Mol. Pharm. 18 (2021) 928–939.
[22] H. Yu, J.S. Kim, D.W. Kim, E.S. Park, Y.S. Youn, F. ud Din, J.O. Kim, S.K. Ku, S. G. Jin, H.-G. Choi, Novel composite double-layered dressing with improved mechanical properties and wound recovery for thermosensitive drug, lactobacillus brevis, Compos. Part B Eng. 225 (2021) 109276.
[23] S. Liu, Y. Gao, D. Zhou, U. Greiser, T. Guo, R. Guo, W. Wang, Biodegradable highly branched poly (β-amino ester) s for targeted cancer cell gene transfection, ACS Biomater Sci. Eng. 3 (2017) 1283–1286.
[24] Y. Tang, Y. Liu, Y. Xie, J. Chen, Y. Dou, Apoptosis of A549 cells by small interfering RNA targeting survivin delivery using poly-β-amino ester/guanidinylated O-carboxymethyl chitosan nanoparticles, Asian, J. Pharm. Sci. 15 (2020) 121–128.
[25] P. Heydari, J. Varshosaz, M. Kharaziha, S.H. Javanmard, Antibacterial and pH-sensitive methacrylate poly-L-arginine/poly (β-amino ester) polymer for soft tissue engineering, J. Mater. Sci. Mater. Med. 34 (2023) 16.
[26] M.T. Khorasani, A. Joorabloo, A. Moghaddam, H. Shamsi, Z. MansooriMoghadam, Incorporation of ZnO nanoparticles into heparinised polyvinyl alcohol/chitosan hydrogels for wound dressing application, Int. J. Biol. Macromol. 114 (2018) 1203–1215.
[27] S. Shi, H. Wu, C. Zhi, J. Yang, Y. Si, Y. Ming, B. Fei, J. Hu, A skin-like nanostructured membrane for advanced wound dressing, Compos. Part B Eng. 250 (2023) 110438.
[28] K.C.M. Leung, T.W. Chow, C.W. Woo, R.K.F. Clark, Tensile, shear and cleavage bond strengths of alginate adhesive, J. Dent. 26 (1998) 617–622.
[29] Y. Zhang, X. Wang, J. Chen, D. Qian, P. Gao, T. Qin, T. Jiang, J. Yi, T. Xu, Y. Huang, Exosomes derived from platelet-rich plasma administration in site mediate cartilage protection in subtalar osteoarthritis, J. Nanobiotechnol. 20 (2022) 1–22.
[30] M.F. Abazari, F. Nejati, N. Nasiri, Z.A.S. Khazeni, B. Nazari, S.E. Enderami, H. Mohajerani, Platelet-rich plasma incorporated electrospun PVA-chitosan-HA nanofibers accelerates osteogenic differentiation and bone reconstruction, Gene 720 (2019) 144096.
[31] S. Tavakoli, H. Mokhtari, M. Kharaziha, A. Kermanpur, A. Talebi, J. Moshtaghian, A multifunctional nanocomposite spray dressing of Kappa-carrageenan-polydopamine modified ZnO/L-glutamic acid for diabetic wounds, Mater. Sci. Eng. C 111 (2020) 110837.
[32] H. Adeli, M.T. Khorasani, M. Parvazinia, Wound dressing based on electrospun PVA/chitosan/starch nanofibrous mats: fabrication, antibacterial and cytocompatibility evaluation and in vitro healing assay, Int. J. Biol. Macromol. 122 (2019) 238–254.
[33] L. Wang, J.P. Stegemann, Thermogelling chitosan and collagen composite hydrogels initiated with β-glycerophosphate for bone tissue engineering, Biomaterials 31 (2010) 3976–3985.
[34] A. Ben Hsouna, R. Ben Saad, W. Dhifi, W. Mnif, F. Brini, Novel non-specific lipid-transfer protein (TdLTP4) isolated from durum wheat: antimicrobial activities and anti-inflammatory properties in lipopolysaccharide (LPS)-stimulated RAW 264.7 macrophages, Microb. Pathog. 154 (2021) 104869.
[35] S. Sadeghi-Soureh, R. Jafari, R. Gholikhani-Darbroud, Y. Pilehvar-Soltanahmadi, Potential of Chrysin-loaded PCL/gelatin nanofibers for modulation of macrophage functional polarity towards anti-inflammatory/pro-regenerative phenotype, J. Drug Deliv. Sci. Technol. 58 (2020) 101802.
[36] C. Gorgun, D. Ceresa, R. Lesage, F. Villa, D. Reverberi, C. Balbi, S. Santamaria, K. Cortese, P. Malatesta, L. Geris, Dissecting the effects of preconditioning with inflammatory cytokines and hypoxia on the angiogenic potential of mesenchymal stromal cell (MSC)-derived soluble proteins and extracellular vesicles (EVs), Biomaterials 269 (2021) 120633.
[37] T.I. Shaheen, M.F. Abdelhameed, S. Zaghloul, A.S. Montaser, In vivo assessment of the durable, green and in situ bio-functional cotton fabrics based carboxymethyl chitosan nanohybrid for wound healing application, Int. J. Biol. Macromol. 209 (2022) 485–497.

[38] A.M. Hawkins, T.A. Milbrandt, D.A. Puleo, J.Z. Hilt, Synthesis and analysis of degradation, mechanical and toxicity properties of poly (β-amino ester) degradable hydrogels, Acta Biomater. 7 (2011) 1956–1964.
[39] Q. Yan, H.-N. Zheng, C. Jiang, K. Li, S.-J. Xiao, EDC/NHS activation mechanism of polymethacrylic acid: anhydride versus NHS-ester, RSC Adv. 5 (2015) 69939–69947.
[40] R. Shakiba-Marani, H. Ehtesabi, A flexible and hemostatic chitosan, polyvinyl alcohol, carbon dot nanocomposite sponge for wound dressing application, Int. J. Biol. Macromol. 224 (2023) 831–839.
[41] M. Gruppuso, F. Iorio, G. Turco, E. Marsich, D. Porrelli, Hyaluronic acid/lactose-modified chitosan electrospun wound dressings–crosslinking and stability criticalities, Carbohydr. Polym. 288 (2022) 119375.
[42] S. Zhang, J. Hou, Q. Yuan, P. Xin, H. Cheng, Z. Gu, J. Wu, Arginine derivatives assist dopamine-hyaluronic acid hybrid hydrogels to have enhanced antioxidant activity for wound healing, Chem. Eng. J. 392 (2020) 123775.
[43] S. Tavakoli, M. Kharaziha, A. Kermanpur, H. Mokhtari, Sprayable and injectable visible-light Kappa-carrageenan hydrogel for in-situ soft tissue engineering, Int. J. Biol. Macromol. 138 (2019) 590–601.
[44] J. Zhou, V. Bhagat, M.L. Becker, Poly (ester urea)-based adhesives: improved deployment and adhesion by incorporation of poly (propylene glycol) segments, ACS Appl. Mater. Interfaces 8 (2016) 33423–33429.
[45] N. Lang, M.J. Pereira, Y. Lee, I. Friehs, N.V. Vasilyev, E.N. Feins, K. Ablasser, E. D. O'Cearbhaill, C. Xu, A. Fabozzo, A blood-resistant surgical glue for minimally invasive repair of vessels and heart defects, Sci. Transl. Med. 6 (2014) (218ra6-218ra6).
[46] N. Annabi, D. Rana, E.S. Sani, R. Portillo-Lara, J.L. Gifford, M.M. Fares, S. M. Mithieux, A.S. Weiss, Engineering a sprayable and elastic hydrogel adhesive with antimicrobial properties for wound healing, Biomaterials 139 (2017) 229–243.
[47] M. Yao, A. Yaroslavsky, F.P. Henry, R.W. Redmond, I.E. Kochevar, Phototoxicity is not associated with photochemical tissue bonding of skin, Lasers Surg. Med. Off. J. Am. Soc. Laser Med. Surg. 42 (2010) 123–131.
[48] F. Jahoor, J.W. Hsu, P. Dwarkanath, M.M. Thame, A.V. Kurpad, L-Arginine production during pregnancy, in: L-Arginine Clin. Nutr, Springer, 2017, pp. 271–284.
[49] T. Liu, G. Liu, J. Zhang, Z. Ding, Y. Li, K. Sigdel, X. Wang, H. Xie, L-arginine based polyester amide/hyaluronic acid hybrid hydrogel with dual anti-inflammation and antioxidant functions for accelerated wound healing, Chin. Chem. Lett. 33 (2022) 1880–1884.
[50] Y. Hussein, E.M. El-Fakharany, E.A. Kamoun, S.A. Loutfy, R. Amin, T.H. Taha, S. A. Salim, M. Amer, Electrospun PVA/hyaluronic acid/L-arginine nanofibers for wound healing applications: nanofibers optimization and in vitro bioevaluation, Int. J. Biol. Macromol. 164 (2020) 667–676.
[51] S. Ray, X. Ju, H. Sun, C.C. Finnerty, D.N. Herndon, A.R. Brasier, The IL-6 trans-signaling-STAT3 pathway mediates ECM and cellular proliferation in fibroblasts from hypertrophic scar, J. Invest. Dermatol. 133 (2013) 1212–1220.
[52] M.B. Witte, A. Barbul, M.A. Schick, N. Vogt, H.D. Becker, Upregulation of arginase expression in wound-derived fibroblasts, J. Surg. Res. 105 (2002) 35–42.
[53] R. Wang, K. Li, L. Sun, H. Jiao, Y. Zhou, H. Li, X. Wang, J. Zhao, H. Lin, L-arginine/nitric oxide regulates skeletal muscle development via muscle fibre-specific nitric oxide/mTOR pathway in chickens, Anim. Nutr. 10 (2022) 68–85.
[54] Z. Feng, Q. Su, C. Zhang, P. Huang, H. Song, A. Dong, D. Kong, W. Wang, Bioinspired nanofibrous glycopeptide hydrogel dressing for accelerating wound healing: a cytokine-free, M2-type macrophage polarization approach, Adv. Funct. Mater. 30 (2020) 2006454.
[55] M. He, L. Sun, X. Fu, S.P. McDonough, C.-C. Chu, Biodegradable amino acid-based poly (ester amine) with tunable immunomodulating properties and their in vitro and in vivo wound healing studies in diabetic rats' wounds, Acta Biomater. 84 (2019) 114–132.
[56] M.A. Ramírez, J. Morales, M. Cornejo, E.H. Blanco, E. Mancilla-Sierpe, F. Toledo, A.R. Beltrán, L. Sobrevia, Intracellular acidification reduces L-arginine transport via system y+ L but not via system y+/CATs and nitric oxide synthase activity in human umbilical vein endothelial cells, Biochim. Biophys. Acta (BBA)-Molecular Basis Dis. 1864 (2018) 1192–1202.
[57] G. Zhang, S. Han, L. Wang, Y. Yao, K. Chen, S. Chen, A ternary synergistic eNOS gene delivery system based on calcium ion and L-arginine for accelerating angiogenesis by maximizing NO production, Int. J. Nanomedicine 17 (2022) 1987.
[58] N. Yamamoto, T. Oyaizu, M. Enomoto, M. Horie, M. Yuasa, A. Okawa, K. Yagishita, VEGF and bFGF induction by nitric oxide is associated with hyperbaric oxygen-induced angiogenesis and muscle regeneration, Sci. Rep. 10 (2020) 1–13.
[59] N. Zhao, W. Yuan, Highly adhesive and dual-crosslinking hydrogel via one-pot self-initiated polymerization for efficient antibacterial, antifouling and full-thickness wound healing, Compos. Part B Eng. 230 (2022) 109525.
[60] X. Han, S. Chen, Z. Cai, Y. Zhu, W. Yi, M. Guan, B. Liao, Y. Zhang, J. Shen, W. Cui, A diagnostic and therapeutic hydrogel to promote vascularization via blood sugar reduction for wound healing, Adv. Funct. Mater. 2213008 (2023).